

**Nonclassicality indicator for the real phase-space distribution functions**Parvin Sadeghi, Siamak Khademi,<sup>\*</sup> and Sadollah Nasiri<sup>†</sup>*Department of Physics, Zanjan University, ZNU, Zanjan, Iran*

(Received 29 October 2009; revised manuscript received 5 April 2010; published 12 July 2010)

Benedict *et al.* and Kenfack *et al.* advocated nonclassicality indicators based on the measurement of negativity of the Wigner distribution functions. These indicators have some applications in quantum mechanics and quantum optics. In this paper we define a nonclassicality indicator in terms of the interference in phase space, which is applicable to some real distribution functions including those of Wigner. As a special case one may reproduce the previous results using our indicator for the Wigner distribution functions. This indicator is examined for cases of the Schrödinger cat state and the thermal states and the results are compared with those obtained by previous methods. It seems that the physical behavior of nonclassicality indicators originates in the uncertainty principle. This is shown by an onto correspondence between these indicators and the uncertainty principle.

DOI: [10.1103/PhysRevA.82.012102](https://doi.org/10.1103/PhysRevA.82.012102)

PACS number(s): 03.65.Ca

**I. INTRODUCTION**

States with the minimum uncertainty are considered to be the classical states in quantum mechanics [1]. These are the quantum states which are the closest ones to the classical states. An earlier attempt to shed some light on the nonclassicality of a quantum state was pioneered by Mandel, who investigated the radiation fields and introduced an indicator measuring the deviation of the photon number statistics from the Poissonian distribution, characteristic of the coherent states [2]. Dodonov presented a review on 75 years of studies about the nonclassical states in quantum optics and the uncertainty relations [3]. The nonclassicality indicators (NCIs) given by Benedict *et al.* [4,5] and Kenfack *et al.* [1], which are not independent, are defined in terms of the volume of the negative part of Wigner distribution functions (WDFs) in the phase space. Some authors have considered the negativity of WDFs to investigate quantum interference and nonclassical effects such as fractional revivals, squeezing, and higher-order squeezing of photon-added coherent states propagating through a Kerr-like medium [6–11]. WDFs corresponding to these states in the instance of fractional revivals were obtained and negativity of the WDFs was assumed as an NCI of the states concerned. Also, Nogues *et al.* [12] have measured WDFs at the origin of the phase space for a single-photon field. Its negative value exhibits the nonclassicality nature of this state.

Although these NCIs apply for a wide set of examples, they have the following inconsistencies.

(i) They are applied for the WDF, which is real and in general has negative values in some regions of the phase space. It can be shown that they are representation dependent and have different behaviors for other distribution functions (DFs).

(ii) The NCIs have zero values for classical states and nonzero values for nonclassical ones. However, the reason for different values of the NCIs has not yet been explored.

(iii) They will be washed out for nonclassical states for which the corresponding WDFs are positive over the available phase space [13].

Dragoman [14] assumes an interference phenomenon to be the source of negativity in the WDFs. Thus, one may define the NCI on the basis of the interference phenomenon in the phase-space picture of the quantum mechanics. In this respect, Jeong and Ralph [13] believe that the interference is responsible for the nonclassical behavior occurring in the thermal state. In contrast, definition of the NCI for non-negative DFs in the phase space according to their negative properties does not mean anything more. For example, for Husimi DFs, which are positive everywhere in the phase space, the interference seems to be more appropriate to indicate nonclassicality.

Here we attempt to remove the aforementioned discrepancies by introducing an NCI based on the interference phenomena displayed by real DFs. Such an indicator would be applicable to different DFs describing the same physical phenomena [15,16].

In Sec. II a brief review of the definition and application of NCIs is presented. In Sec. III our NCI is defined. In Secs. IV and V this NCI is applied to the Schrödinger cat state (SCS) and the thermal state for WDFs, Husimi DFs, and Rivier DFs, respectively. In Sec. VI the correspondence behavior between the new NCI and the uncertainty principle is explored, and Sec. VII is devoted to the conclusions.

**II. VIOLATION OF NEGATIVITY AS A NONCLASSICALITY INDICATOR**

Quantum mechanical DFs, unlike classical probability distributions, which must be real and non-negative, can be either negative or complex functions of the phase-space variables. Despite the fact that some DFs, like those of Husimi [17] and Rivier, are real and positive, some are real and (or) negative (e.g., WDFs [18]), and others are complex (e.g., that of Kirkwood [19]). The negativity of WDFs is interpreted as a nonclassical effect [1,4,11]. According to this property the parameter  $\delta$ , defined as

$$\begin{aligned} \delta &= \int_{-\infty}^{\infty} [|W(q,p)| - W(q,p)] dq dp \\ &= \int_{-\infty}^{\infty} |W(q,p)| dq dp - 1, \end{aligned} \quad (1)$$

<sup>\*</sup>skhademi@znu.ac.ir<sup>†</sup>Also at Institute for Advanced Studies in Basic Science, IASBS, Zanjan, Iran.

by Kenfack and Życzkowski [1], is considered as the NCI. By definition,  $\delta$  is 0 for coherent states, for which the Wigner functions are non-negative.  $\delta$  is related to the indicator  $\nu$ , defined by Benedict *et al.* [4,5], as a measure of the nonclassicality of a quantum state as follows:

$$\nu = \frac{2I_-}{2I_- + 1}, \quad 0 \leq \nu < 1, \quad (2)$$

where  $I_-$  is the module of the integrals over the negative domains of the DF. By Eq. (1) and normalization conditions of the WDFs, one gets  $\delta = 2I_-$ . Thus a simple relation can be obtained between the two quantities as  $\nu = \delta(1 + \delta)^{-1}$ , indicating their equivalence. Later, because of this equivalence, we just focus on  $\delta$ .

Owing to the equivalence of the different DFs [15], a physical effect assigned to the negativity of a DF should not be removed from one DF to another. Therefore, how does this effect appear for the different DFs, especially those which are always positive?

Like WDFs, Rivier DFs are real and become negative in some parts of the phase space. However,  $\delta$  behaves differently for WDFs and Rivier DFs. This different behavior is plotted for the SCS in Fig. 1.

The SCS is defined as a coherent superposition of two Gaussian wave packets [6] separated by a peak-to-peak distance of  $q_0$  in the configuration space. The wave function of such a state reads

$$\psi(q) = \frac{N(p_0, q_0)}{\sqrt{2}} [\phi^+(q) + \phi^-(q)], \quad (3)$$

where

$$\phi^\pm(q) = \left( \frac{m\omega}{\pi\hbar} \right)^{1/4} \exp \left[ -\frac{m\omega}{2\hbar} (q \pm q_0)^2 + i \frac{p_0}{\hbar} (q \pm q_0) \right]. \quad (4)$$

For the sake of simplicity we set  $m = \hbar = \omega = 1$ . In Eq. (3),  $N(p_0, q_0) = [1 + \cos(2q_0 p_0) e^{-q_0^2}]^{-1/2}$  is a constant of normalization. From Eqs. (3) and (4) one obtains the WDFs as

$$W(q, p) = \frac{1}{\pi} \int_{-\infty}^{\infty} e^{2ipx} dx [\phi^+(q-x)\phi^{+*}(q+x) + \phi^-(q-x)\phi^{-*}(q+x) + \phi^+(q-x)\phi^{-*}(q+x) + \phi^-(q-x)\phi^{+*}(q+x)]. \quad (5)$$

Equation (5) contains four terms. Diagonal terms, that is, the first and second terms, denoted  $W_{11}$  and  $W_{22}$ , are caused by the coherent states localized in  $+q_0$  (or  $-q_0$ ) and the cross terms, denoted  $W_{12} + W_{21} = W_{\text{int}}$ , are the interference terms. Thus

$$W(q, p) = W_{11}(q, p) + W_{22}(q, p) + W_{\text{int}}(q, p), \quad (6)$$

where

$$W_{11}(q, p) = \frac{N^2(p_0, q_0)}{2\pi} \exp[-(q + q_0)^2 - (p - p_0)^2], \quad (7)$$

$$W_{22}(q, p) = \frac{N^2(p_0, q_0)}{2\pi} \exp[-(q - q_0)^2 - (p - p_0)^2],$$

and

$$W_{\text{int}}(q, p) = \frac{N^2(p_0, q_0)}{\pi} \exp[-q^2 - (p - p_0)^2] \cos(2q_0 p). \quad (8)$$

Separation of the WDF into three parts will help us to introduce a new NCI.

Now it is useful to give some interpretation for  $\delta$  using the WDF for the SCS. The first and second terms in Eq. (6) are positive and have no oscillations. But the third term (interference term) is oscillatory and would assume negative values. All oscillations and corresponding negativities vanish at  $q_0 \rightarrow 0$ . Thus, there is a correspondence between the negativity and the interference of the SCS.

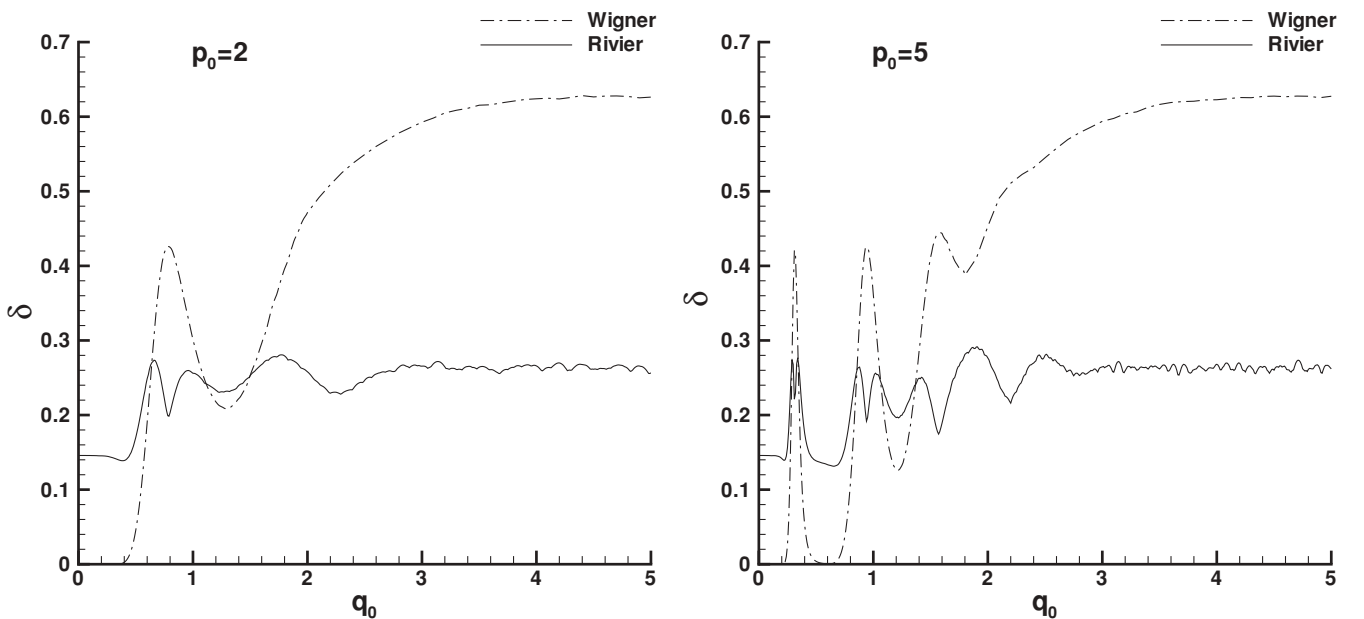


FIG. 1. Indicator  $\delta$  for the Wigner and Rivier DFs of the SCS versus the separation distance  $q_0$  for several values of  $p_0$  as labeled in each plot.  $\delta$  shows different behavior in the Wigner and Rivier representations.  $q_0$  and  $p_0$  are dimensionless parameters.

For states occupied at the limit of  $q_0 \rightarrow \infty$ , the cosine term in Eq. (8) rapidly oscillates, independently of  $p_0$ , and a crude approximation  $|\cos(q_0 p_0)| \simeq 1$  gives an explicit upper bound for  $\delta$ , that is,  $\delta < 1$ .

### III. INTERFERENCE AS AN INDICATOR OF NONCLASSICALITY

Some authors, like Dragoman [14], believe that the interference in the Wigner representation is the source of negativity of the WDF. Any DFs,  $F(p, q)$ , which are made by superposition of two (or more) state functions can be separated into different terms denoted  $F_{ij}$ , where  $i$  and  $j$  enumerate the state functions and the diagonal (cross) terms correspond to  $i = j$  ( $i \neq j$ ). For example, in Eq. (6) one has  $F_{12} = W_{12}$ ,  $F_{21} = W_{21}$ ,  $F_{11} = W_{11}$ , and  $F_{22} = W_{22}$ , therefore

$$F(p, q) = \sum_{ij} F_{ij}. \quad (9)$$

The individual terms in the real DFs may be imaginary, while their sum should be real.

Let us define an NCI,  $\eta$ , as

$$\eta = \frac{\sum_{ij} \int_{-\infty}^{\infty} [|f_{ij}| - f_{ij}] dq dp}{\sum_{ij} \int_{-\infty}^{\infty} [|f_{ij}| + f_{ij}] dq dp}, \quad (10)$$

where  $f_{ij}(p, q) = \text{Re}[F_{ij}(p, q)]$  and the integrals in the nominator are the negative parts of  $f_{ij}$ . The denominator is arranged to keep  $\eta$  at  $0 \leq \eta < 1$ . If  $\eta = 0$ , the corresponding quantum state is the nearest one to the classical state. Other values of  $\eta$  indicate departure from the classical state. As examples, we apply  $\eta$  for a few well-known real DFs, that is, WDFs, Husimi DFs, and Rivier DFs. We rewrite  $\eta$  as

$$\eta = \frac{\sum_{ij} \Delta_{ij}}{\sum_{ij} \Delta_{ij} + 2}, \quad (11)$$

where

$$\Delta_{ij} = \int_{-\infty}^{\infty} [|f_{ij}(q, p)| - f_{ij}(q, p)] dq dp. \quad (12)$$

It is important to note that  $\eta$  is defined as a superposition of the negative parts of the individual terms, while  $\delta$  is defined as the negative parts of the superposition of those terms. This is the key point in the definition of  $\eta$  that originates in the interference phenomenon. In contrast, for positive definite DFs (e.g., Husimi DFs for all systems or WDFs for the thermal state),  $\eta \geq 0$ , while  $\delta = 0$ . Thus, according to  $\delta$ , all quantum states in the Husimi representation are classical states, which is not correct at all.

As a special case, for  $i = j = 1$ ,  $f_{ij} = f_{11} = f$ ,  $\eta$  becomes

$$\eta = \frac{\int_{-\infty}^{\infty} [|f| - f] dq dp}{\int_{-\infty}^{\infty} [|f| + f] dq dp} = \frac{\Delta}{2 + \Delta}. \quad (13)$$

For WDFs one has  $F = W$ ,  $\Delta = \delta$ , and

$$\eta = \frac{\delta}{2 + \delta} = \frac{\nu}{2 - \nu}. \quad (14)$$

Thus, the role of  $\delta$  or  $\nu$  emerges as a special case of  $\eta$  for WDFs.

### IV. APPLICATION TO THE SCHRÖDINGER CAT STATE

The variation of  $\delta$  for the SCS in the Wigner and the Rivier representations obtained in Sec. II is plotted in Fig. 1. Clearly this parameter vanishes for the Husimi representation. Now we study the behavior of  $\eta$  for the SCS in the Husimi, Rivier, and Wigner representations. For the WDF,  $\eta$  can be obtained using Eqs. (5)–(10). The results are plotted in Fig. 2, which shows a behavior similar to that of  $\delta$ .

The Rivier DF is given by

$$R(q, p) = \frac{1}{2}[\chi(q, p) + \chi^*(q, p)], \quad (15)$$

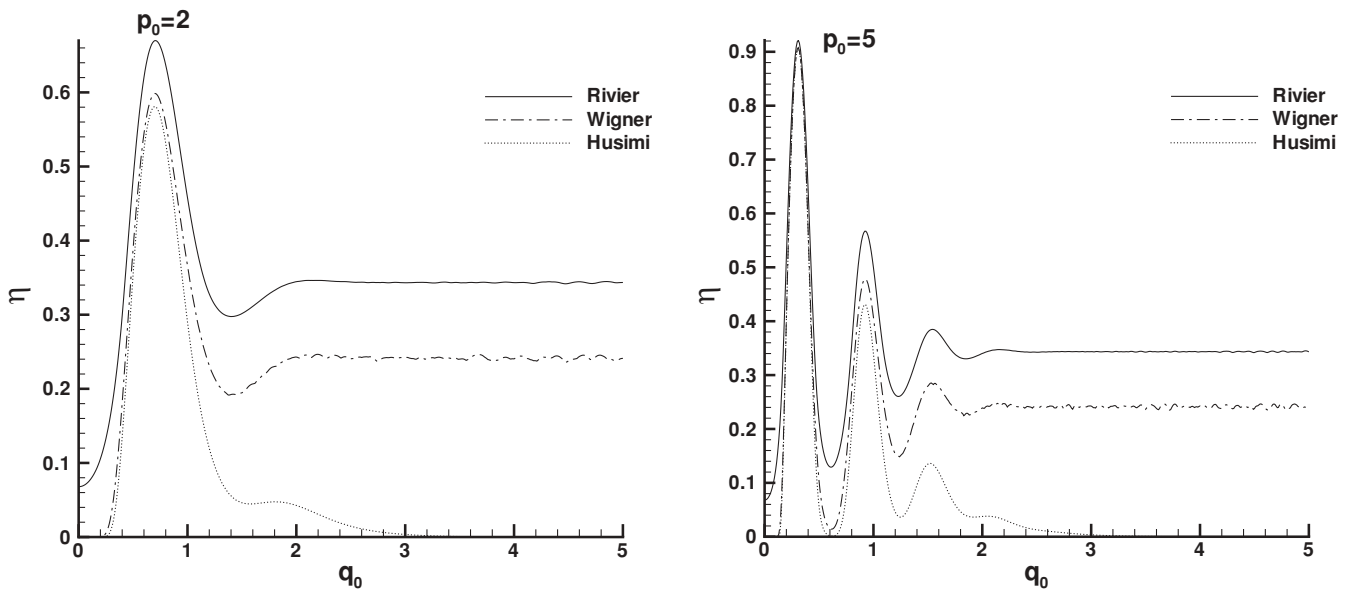


FIG. 2. Indicator  $\eta$  for the Wigner, Husimi, and Rivier DFs of the SCS versus the separation distance  $q_0$  for different  $p_0$  values.  $\eta$  shows similar behavior, demonstrating the equivalence of these representations in the phase space.

which is the real part of the Kirkwood DF,

$$\chi(q, p) = \frac{1}{\sqrt{2\pi}} \psi(q) \Phi^*(p) e^{-iqp}. \quad (16)$$

In Eq. (16),  $\Phi^*(p) = \varphi^+(p) + \varphi^-(p)$  is the state function in the momentum space corresponding to  $\psi(q)$  in the configuration space. If the system is made by the superposition of two states, one obtains the Rivier DF as

$$R(q, p) = R^+(q, p) + R^-(q, p) + R_{\text{int}}(q, p), \quad (17)$$

where

$$\begin{aligned} R^+(q, p) &= \text{Re} \left\{ \frac{N^2(q_0, p_0)}{2\pi\sqrt{2}} [\phi^+(q)\varphi^{+*}(p)] e^{-ipq} \right\}, \\ R^-(q, p) &= \text{Re} \left\{ \frac{N^2(q_0, p_0)}{2\pi\sqrt{2}} [\phi^-(q)\varphi^{-*}(p)] e^{-ipq} \right\}, \\ R_{\text{int}}(q, p) &= \text{Re} \left\{ \frac{N^2(q_0, p_0)}{2\pi\sqrt{2}} [\phi^+(q)\varphi^{-*}(p) \right. \\ &\quad \left. + \phi^-(q)\varphi^{+*}(p)] e^{-ipq} \right\}. \end{aligned} \quad (18)$$

Thus the Rivier DF for the SCS (4) is given by

$$\begin{aligned} R &= \frac{N^2(q_0, p_0)}{2\pi\sqrt{2}} \left\{ e^{-\frac{1}{2}(q-q_0)^2 - \frac{1}{2}(p-p_0)^2} \cos[(p-p_0)(q-q_0)] \right. \\ &\quad + e^{-\frac{1}{2}(q+q_0)^2 - \frac{1}{2}(p-p_0)^2} \cos[(p-p_0)(q+q_0)] \\ &\quad + e^{-\frac{1}{2}(q-q_0)^2 - \frac{1}{2}(p+p_0)^2} \cos[q_0(p+p_0) + q(p-p_0)] \\ &\quad \left. + e^{-\frac{1}{2}(q+q_0)^2 - \frac{1}{2}(p+p_0)^2} \cos[q_0(p+p_0) - q(p-p_0)] \right\}. \end{aligned} \quad (19)$$

In this case

$$\begin{aligned} R^\pm(q, p) &= \frac{N^2(q_0, p_0)}{2\pi\sqrt{2}} e^{-\frac{1}{2}(q \pm q_0)^2 - \frac{1}{2}(p-p_0)^2} \\ &\quad \times \cos[(p-p_0)(q \pm q_0)], \end{aligned}$$

$$\begin{aligned} R_{\text{int}}(q, p) &= \frac{N^2(q_0, p_0)}{2\pi\sqrt{2}} \left\{ e^{-\frac{1}{2}(q-q_0)^2 - \frac{1}{2}(p-p_0)^2} \right. \\ &\quad \times \cos[q_0(p+p_0) + q(p-p_0)] \\ &\quad + e^{-\frac{1}{2}(q+q_0)^2 - \frac{1}{2}(p-p_0)^2} \cos[q_0(p+p_0) \\ &\quad \left. - q(p-p_0)] \right\}. \end{aligned} \quad (20)$$

As mentioned before,  $\delta$  vanishes in the Husimi representation, giving no information about the nonclassicality of the state in this representation. The Husimi positive DF is obtained by a Gaussian smoothing of the WDF [15] as

$$H(q, p) = \frac{1}{\pi} \int_{-\infty}^{\infty} dq' dp' W(q', p') e^{-(q-q')^2 - (p-p')^2}. \quad (21)$$

Using Eq. (5) in Eq. (21), the Husimi DF can be obtained for the SCS as

$$H = H^+ + H^- + H_{\text{int}}, \quad (22)$$

where

$$\begin{aligned} H^\pm &= \frac{N^2(p_0, q_0)}{4\pi} \exp \left[ -\frac{1}{2}(q \pm q_0)^2 - \frac{1}{2}(p-p_0)^2 \right], \\ H_{\text{int}} &= H^{+-} + H^{-+} = \frac{N^2(p_0, q_0)}{2\pi} e^{-\frac{1}{2}[q^2 + q_0^2 + (p-p_0)^2]} \\ &\quad \times \cos[q_0(p+p_0)]. \end{aligned} \quad (23)$$

Equation (23) shows that the diagonal terms are positive, while the cross terms are negative, in some regions of the phase space. Eqs. (1), (10), and (19)–(23) give  $\delta$  and  $\eta$ , which are plotted in Figs. 1 and 2, respectively. Note that (i) in Fig. 1 the behavior (i.e., the variation and the location of minima and maxima) of  $\delta$  is different for the Wigner, Rivier, and Husimi ( $\delta = 0$ ) representations, leaving  $\delta$  as a representation-dependent parameter; and (ii) in Fig. 2 the behavior of  $\eta$  is similar for the Wigner, Rivier, and Husimi representations.  $\delta$  and  $\eta$  are also plotted in Figs. 3 and 4 in terms of  $p_0$  for  $q_0 = 1$  and 2. It is shown that, in contrast to

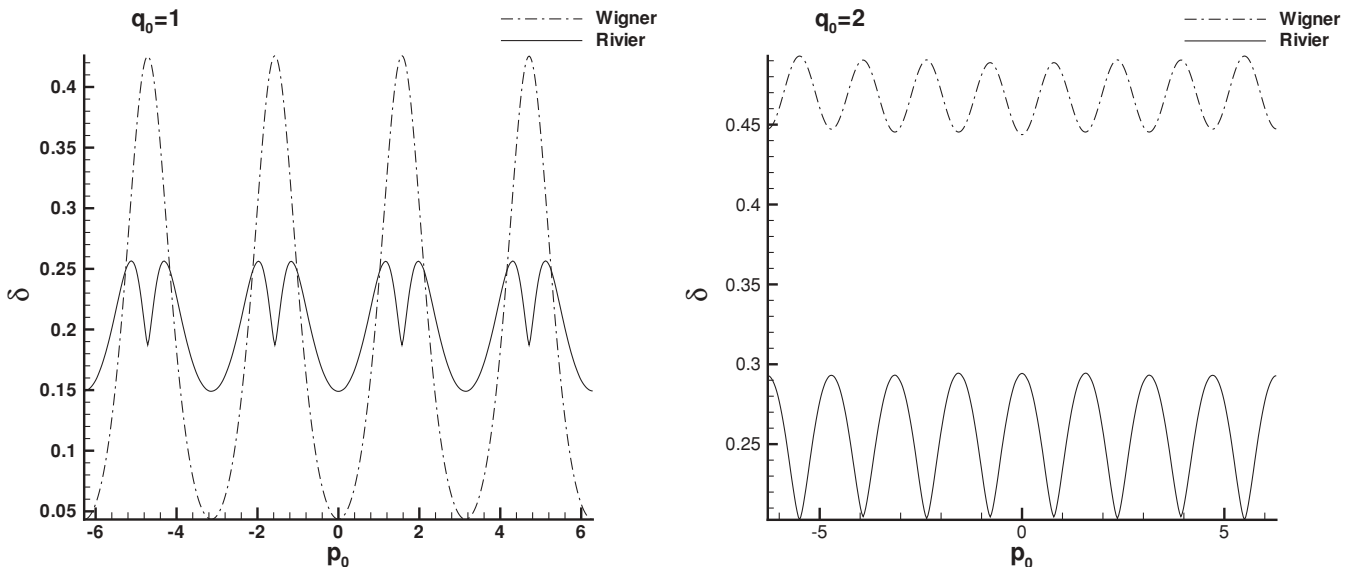


FIG. 3.  $\delta$  of the Wigner and Rivier DFs for the SCS versus  $p_0$  for different  $q_0$  values.  $\delta$  shows different behaviors.

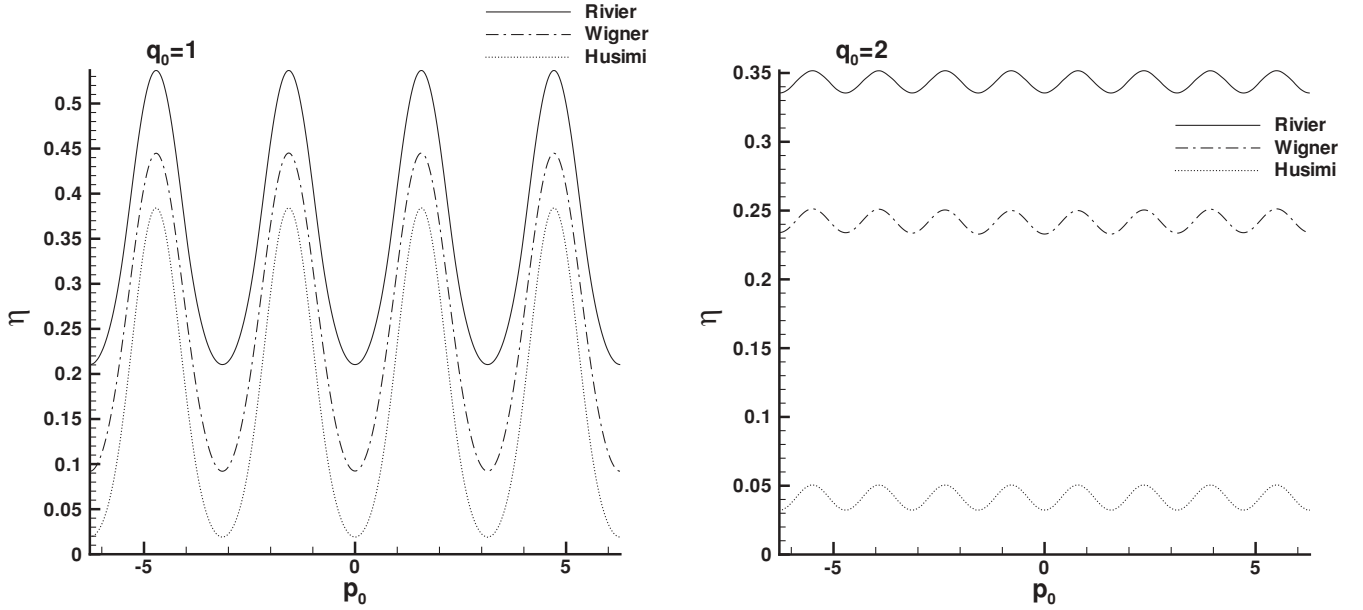


FIG. 4.  $\eta$  of the Wigner, Husimi, and Rivier DFs for the SCS versus  $p_0$  for different  $q_0$  values.  $\eta$  shows similar behavior, demonstrating the equivalence of these representations in the phase space.

$\delta$ ,  $\eta$  again has a similar behavior in the different phase-space representations.

## V. APPLICATION TO THE THERMAL STATE

Let us consider a two-mode harmonic oscillator interacting with an electromagnetic field in a cavity. A displaced thermal state can be defined as [13,20]

$$\rho^{\text{th}}(V, d) = \int d^2\alpha P^{\text{th}}(V, d) |\alpha\rangle\langle\alpha|, \quad (24)$$

where  $|\alpha\rangle$  is a coherent state of amplitude  $\alpha$  and

$$P^{\text{th}}(V, d) = \frac{2}{\pi(V-1)} e^{-\frac{2|\alpha-d|^2}{V-1}}, \quad (25)$$

with dimensionless variance  $V$  and displacement  $d$  in the phase space.  $d$  varies with the intensity of the field and  $V$  depends on the temperature  $T$  by  $e^{\hbar\nu/kT} = (V+1)/(V-1)$ . We consider an interaction of the thermal state with a microscopic superposition of a two-mode harmonic oscillator of ground ( $|0\rangle$ ) and first excited ( $|1\rangle$ ) states given by

$$|\psi\rangle = \frac{1}{\sqrt{2}}(|0\rangle + |1\rangle). \quad (26)$$

The interaction Hamiltonian  $H_\lambda = \lambda \hat{a}^\dagger \hat{a} \hat{b}^\dagger \hat{b}$ , which corresponds to the Kerr nonlinearity, yields the evolution of the system through the interacting density operator as follows:

$$\begin{aligned} \rho^{\text{th}} = & \frac{1}{2} \int d^2\alpha P^{\text{th}}(V, d) \{ |0\rangle\langle 0| \otimes |\alpha\rangle\langle\alpha| \\ & + |1\rangle\langle 0| \otimes |\alpha e^{i\phi}\rangle\langle\alpha| \\ & + |0\rangle\langle 1| \otimes |\alpha\rangle\langle\alpha e^{i\phi}| \\ & + |1\rangle\langle 1| \otimes |\alpha e^{i\phi}\rangle\langle\alpha e^{i\phi}| \}, \end{aligned} \quad (27)$$

where  $a^\dagger$  ( $a$ ) and  $b^\dagger$  ( $b$ ) are the creation (annihilation) operators of the oscillator and field, respectively, and  $\phi = \lambda t$ .

The WDF corresponding to Eq. (27) is

$$\begin{aligned} W(p, q) = & N \{ W^{\text{th}}(\alpha; d) + 2\alpha V^c(\alpha; d) + 2[\alpha V^c(\alpha; d)]^* \\ & + (4|\alpha|^2 - 1)W^{\text{th}}(\alpha; d e^{i\phi}) \}, \end{aligned} \quad (28)$$

where  $p$  and  $q$  are the imaginary and the real parts of  $\alpha$ , respectively. In Eq. (28) one has

$$W^{\text{th}}(p, q; d) = \frac{2}{\pi V} \exp\left[-\frac{(q - \sqrt{2}d)^2 + p^2}{V}\right], \quad (29)$$

$$\begin{aligned} W^{\text{th}}(p, q; d e^{i\phi}) = & \frac{2}{\pi V} \exp\left\{-\frac{1}{V}[(q - \sqrt{2}d \cos \phi)^2 \right. \\ & \left. + (p - \sqrt{2}d \sin \phi)^2]\right\}, \end{aligned} \quad (30)$$

$$\begin{aligned} V^c(p, q; d) = & \frac{2}{\pi JK} \exp\left[-\frac{2d^2}{K}(1 - e^{i\phi}) - \frac{1}{2J}(q^2 + p^2)\right] \\ & + \frac{\sqrt{2}qd}{JK}(1 + e^{i\phi}) - \frac{4d^2 e^{i\phi}}{JK^2}, \end{aligned} \quad (31)$$

where  $K = 2 + (V-1)(1 - e^{i\phi})$ ,  $J = (\sin \phi/2 + iV \cos \phi/2)/(2V \sin \phi/2 + 2i \cos \phi/2)$  and the normalization factor is  $N = \{4 + \frac{4}{K} \exp[-\frac{2d^2}{K}(1 - e^{i\phi})] + \frac{4}{K^*} \exp[-\frac{2d^2}{K^*}(1 - e^{-i\phi})]\}^{-1}$ .

One may obtain the Husimi DF corresponding to Eq. (27) as

$$\begin{aligned} H(p, q) = & H^{\text{th}}(p, q; d) + H^c(p, q; d) \\ & + [H^c(p, q; d)]^* + H^{\text{th}}(p, q; d e^{i\phi}), \end{aligned} \quad (32)$$

where

$$H^{\text{th}}(p, q; d) = \frac{2N}{\pi(V+1)} \exp\left[-\frac{(q - \sqrt{2}d)^2 + p^2}{V+1}\right], \quad (33)$$

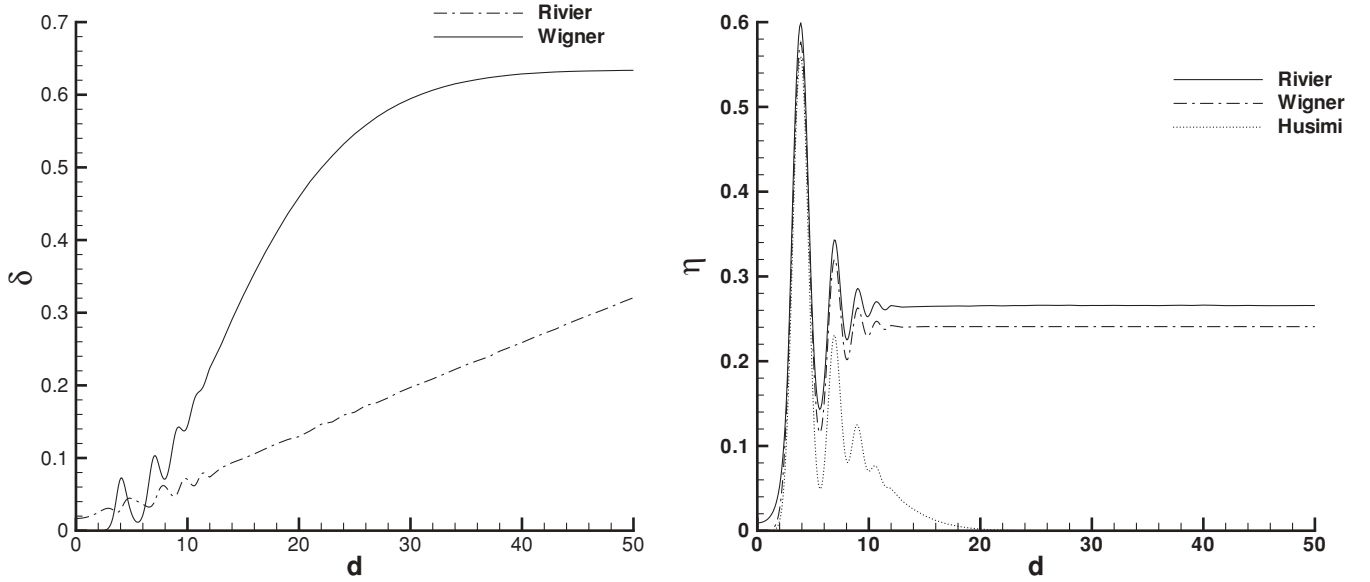


FIG. 5. Left: The different behavior of  $\delta$  for the Wigner and the Rivier representations of the thermal state, where  $\phi = \pi/16$  and  $V = 2$ , while it vanishes for the Husimi representation. Right: The nonclassical indicator  $\eta$  shows similar behavior for the Wigner, Rivier, and Husimi representations for the thermal state with the same  $\phi$  and  $V$ .

$$H^{\text{th}}(p, q; de^{i\phi}) = \frac{2N}{\pi(V+1)} \exp\left[-\frac{(q - \sqrt{2}d \cos \phi)^2 + (p - \sqrt{2}d \sin \phi)^2}{V+1}\right], \quad (34)$$

$$H^c(p, q; d) = \frac{2N}{\pi(2J+1)K} \exp\left[-\frac{2d^2}{K}(1 - e^{i\phi}) - \frac{1}{(2J+1)}(p^2 + q^2)\right] \quad (35)$$

$$\times \exp\left[\frac{2\sqrt{2}qd}{(2J+1)K}(1 + e^{i\phi}) + i\frac{2\sqrt{2}qd}{(2J+1)K}(1 - e^{i\phi}) - \frac{8d^2 e^{i\phi}}{(2J+1)K^2}\right]. \quad (36)$$

Further, the Rivier DF corresponding to Eq. (27) is

$$R(p, q) = R^{\text{th}}(p, q; d) + R^c(p, q; d) + [R^c(p, q; d)]^* + R^{\text{th}}(p, q; de^{i\phi}), \quad (37)$$

where

$$R^{\text{th}}(p, q; d) = \frac{2N}{\pi\sqrt{V^2+1}} \exp\left\{-\frac{V}{V+1}\left[(q - \sqrt{2}d)^2 + p^2 - i\frac{2p(q + \sqrt{2}d)}{V}\right]\right\}, \quad (38)$$

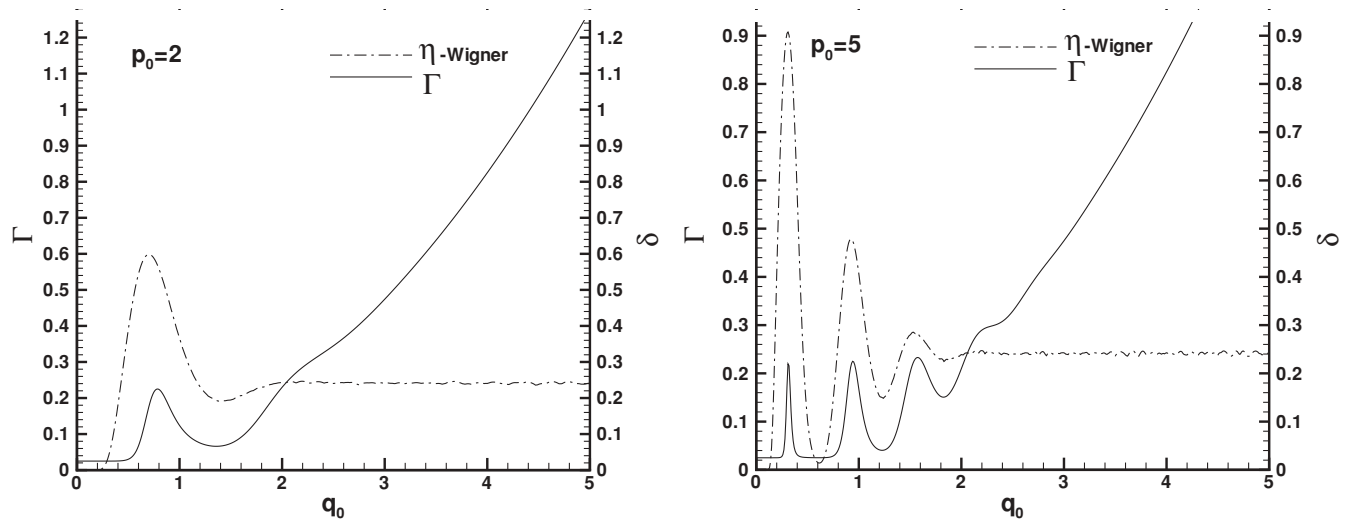


FIG. 6. A comparison between  $\Gamma$  and  $\eta$  versus  $q_0$  in the Wigner representation for  $p_0 = 2$  and 5. Except for large  $q_0$  values, they show a similar behavior.

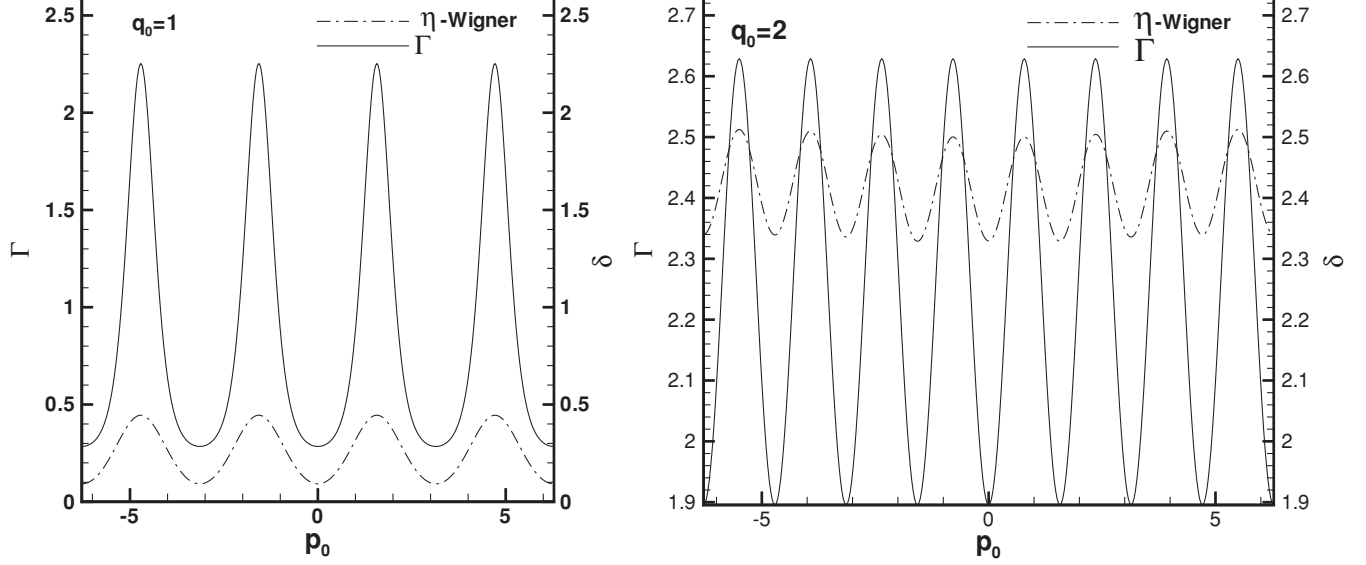


FIG. 7. The similar behavior of dimensionless  $\Gamma$  and  $\eta$  versus  $p_0$  in the Wigner representation for  $q_0 = 1$  and 2. Note that  $\eta$  is plotted out of scale for  $q_0 = 2$ , to have  $\Gamma$  and  $\eta$  in the same plot.

$$\begin{aligned}
 R^{\text{th}}(p, q; d e^{i\phi}) &= \frac{2N}{\pi \sqrt{V^2 + 1}} \exp \left\{ -\frac{V}{V^2 + 1} (q^2 + p^2) \right. \\
 &+ \frac{2\sqrt{2}pd}{V^2 + 1} (i \cos \phi + V \sin \phi) \\
 &+ \frac{2\sqrt{2}qd}{V^2 + 1} (i \sin \phi + V \cos \phi) \\
 &\left. - \frac{2d^2}{V^2 + 1} [(V + i \sin(2\phi)) - i \frac{2pq}{V^2 + 1}] \right\}, \quad (39)
 \end{aligned}$$

$$\begin{aligned}
 R^c(p, q; d) &= \frac{2N}{\pi K \sqrt{4J^2 + 1}} \\
 &\times \exp \left[ -\frac{2d^2}{K} (1 - e^{i\phi}) - \frac{2J}{4J^2 + 1} (p^2 + q^2) \right] \\
 &\times \exp \left\{ \frac{2\sqrt{2}qd}{(4J^2 + 1)K} [2J(1 + e^{i\phi}) - (1 - e^{i\phi})] \right\} \\
 &\times \exp \left\{ i \frac{2\sqrt{2}pd}{(4J^2 + 1)K} [2J(1 - e^{i\phi}) + (1 + e^{i\phi})] \right\} \\
 &\times \exp \left[ -\frac{4d^2(1 - e^{2i\phi} - 4J e^{i\phi})}{(4J^2 + 1)K^2} \right]. \quad (40)
 \end{aligned}$$

Using Eqs. (28)–(40) one may calculate  $\delta$  and  $\eta$  in Eqs. (1) and (10). The behavior of  $\delta$  is shown on the left-hand side of Fig. 5 for the Wigner and Rivier representations, while it vanishes for the Husimi representation.  $\delta$  has a different behavior in terms of variation of  $d$  for the different representations. But the right-hand side in Fig. 5 shows a similar behavior of  $\eta$  as a function of  $d$  for those representations in the phase space.

## VI. UNCERTAINTY PRINCIPLE AND NONCLASSICALITY INDICATOR

Now we are in a position to think about the physical interpretation of  $\eta$ . The inherent uncertainty in the simultaneous

measurement of the conjugate variables has a quantum origin. Thus, it is reasonable that the uncertainty is related to the NCI  $\eta$ . Let us define the uncertainty parameter as follows:

$$\Gamma = (\Delta q)^2 (\Delta p)^2. \quad (41)$$

It can be shown that for the SCS the uncertainty  $\Gamma$  is in terms of  $p_0$  and  $q_0$  and that it is independent of representations. In Fig. 6  $\Gamma$  and  $\eta$  in the Wigner representation are plotted versus  $q_0$  for different  $p_0$ . It is seen that, except for the large  $q_0$ ,  $\Gamma$  and  $\eta$  have similar behavior. Thus one finds an onto relation between  $\eta$  and  $\Gamma$ . Deviation of  $\eta$  and  $\Gamma$  for larger  $q_0$  arises from the inherent nature of the SCS such that the constituent coherent states are separated by  $q_0$ .

Furthermore, the behavior of  $\eta$  for the Wigner representation and  $\Gamma$  are plotted in Fig. 7 in terms of  $p_0$  for

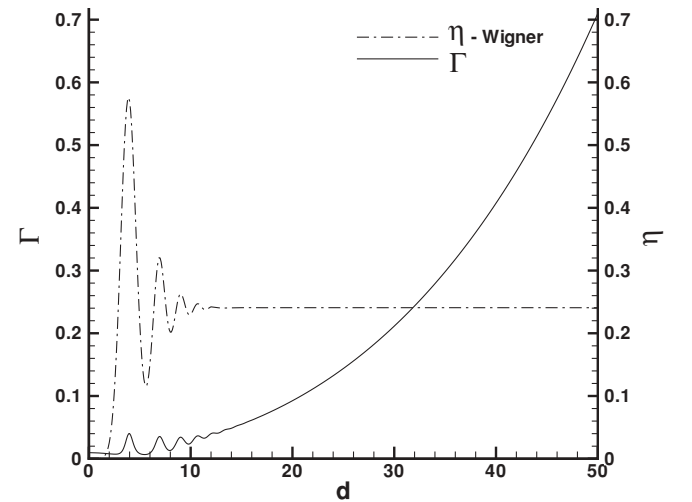


FIG. 8. The similarity behavior of  $\Gamma$  and  $\eta$  versus  $d$  in the Wigner representation for  $V = 2$  and  $\phi = \pi/16$ .

$q_0 = 1$  and 2, showing the same behavior as before. Thus, the relation between  $\Gamma$  and  $\eta$  allows one to have a quantitative interpretation of NCI, that is, a system with higher  $\eta$  has higher quantum mechanical uncertainty, and vice versa. The same interpretation is satisfied for  $\delta$ , however, according to Figs. 2 and 4, in contrast to  $\delta$ ,  $\eta$  has a similar behavior in the other real representations as well.

The behavior of the  $\eta$  and uncertainty  $\Gamma$  for the thermal state is plotted in Fig. 8. It is clear that the correspondence of the functional behavior of  $\Gamma$  and  $\eta$  for the SCS still exists for that of  $\Gamma$  and  $\eta$  calculated for the thermal state as well.

## VII. CONCLUSIONS

The NCIs already defined are applied only to the Wigner representation of the phase-space quantum mechanics. They do not show similar behavior when applied to the other representations. For example, the indicator  $\delta$  introduced by Kenfack *et al.* has different behavior in the different representations as shown in Figs. 1 and 3. To indicate the nonclassicality of a

quantum state in other representations with real DFs, we define an indicator based on the oscillatory nature of these DFs. The idea was proposed first by Dragoman as an inherent quantum interference signature [21]. The behavior of the NCI defined in such a way is representation independent. As illustrative examples it is worked out for the Wigner, Husimi, and Rivier representations for the cases of the SCS and the thermal state. The results plotted in Figs. 2, 4, and 5 show the similar behavior of  $\eta$  for the aforementioned representations. Another result is the relation between the NCI and the uncertainty principle as a fundamental principle of quantum mechanics. The relation between  $\eta$  and the uncertainty principle explored for the SCS and the thermal state are shown in Figs. 6–8, emphasizing the similar behavior of  $\eta$  and  $\Gamma$  in the different representations.

## ACKNOWLEDGMENT

We would like to thank A. H. Darooneh for useful conversations and comments.

- 
- [1] A. Kenfack and K. Życzkowski, *J. Opt. B* **6**, 396 (2004).
  - [2] L. Mandel, *Opt. Lett.* **4**, 205 (1979).
  - [3] V. V. Dodonov, *J. Opt. B* **4**, R1 (2002).
  - [4] M. G. Benedict and A. Czirják, *Phys. Rev. A* **60**, 4034 (1999).
  - [5] P. Faldi, A. Czirják, B. Molnár, and M. G. Benedict, *Opt. Express* **10**, 376 (2002).
  - [6] W. P. Schleich, *Quantum Optics in Phase Space* (Wiley-VCH, Weinheim, 2001).
  - [7] I. Białynicki-Birula, M. A. Cirone, J. P. Dahl, M. Fedorov, and W. P. Schleich, *Phys. Rev. Lett.* **89**, 060404 (2002).
  - [8] J. P. Dahl, A. Wolf, and W. P. Schleich, *Fortschr. Phys.* **52**, 1118 (2004).
  - [9] D. F. Mundarain and J. Stephany, *J. Phys. A* **37**, 3869 (2004).
  - [10] M. Suda, *Quantum Interferometry in Phase Space Theory and Applications* (Springer-Verlag, Berlin, 2006).
  - [11] C. Sudheesh, S. Lakshmibala, and V. Balakrishnan, *J. Opt. B* **7**, S728 (2005).
  - [12] G. Nogues, A. Rauschenbeutel, S. Osnaghi, P. Bertet, M. Brune, J. M. Raimond, S. Haroche, L. G. Lutterbach, and L. Davidovich, *Phys. Rev. A* **62**, 054101 (2000).
  - [13] H. Jeong and T. C. Ralph, *Phys. Rev. Lett.* **97**, 100401 (2006).
  - [14] D. Dragoman, *J. Opt. Soc. Am. A* **17**, 2481 (2000).
  - [15] Lee Hai-Woong, *Phys. Rep.* **259**, 147 (1995).
  - [16] M. Hillery, R. F. O’Connell, M. O. Scully, and E. P. Wigner, *Phys. Rep.* **106**, 121 (1984).
  - [17] K. Husimi, *Proc. Phys. Math. Soc. Japan* **22**, 264 (1940).
  - [18] E. P. Wigner, *Phys. Rev.* **40**, 749 (1932).
  - [19] J. G. Kirkwood, *Phys. Rev.* **44**, 31 (1933).
  - [20] D. F. Walls and G. J. Milburn, *Quantum Optics* (Springer-Verlag, Berlin, 1994).
  - [21] D. Dragoman, *J. Opt. Soc. Am. A* **17**, 2481 (2002).